# JOC *The Journal of Organic Chemistry*

# Cofactor-Mediated Nucleophilic Substitution Catalyzed by a Self-Assembled Holoenzyme Mimic

Courtney Ngai,[†] Paul M. Bogie,[†] Lauren R. Holloway, Phillip C. Dietz, Leonard J. Mueller, and Richard J. Hooley*[ORCID]

Department of Chemistry, University of California—Riverside, Riverside, California 92521, United States

**S** *Supporting Information*

**ABSTRACT:** A self-assembled $Fe_4L_6$ cage is capable of co-encapsulating multiple carboxylic acid containing guests in its cavity, and these acids can act as cofactors for cage-catalyzed nucleophilic substitutions. The kinetics of the substitution reaction depend on the size, shape, and binding affinity of each of the components, and small structural changes in guest size can have large effects on the reaction. The host is quite promiscuous and is capable of binding multiple guests with micromolar binding affinities while retaining the ability to effect turnover and catalysis. Substrate binding modes vary widely, from simple 1:1 complexes to 1:2 complexes that can show either negative or positive cooperativity, depending on the guest. The molecularity of the dissociative substitution reaction varies, depending on the electrophile leaving group, acid cofactor, and nucleophile size: small changes in the nature of substrate can have large effects on reaction kinetics, all controlled by selective molecular recognition in the cage interior.
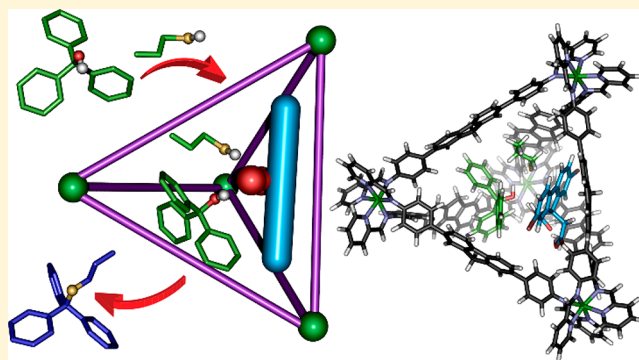
## ■ INTRODUCTION

The scope of enzymatic reactions is widely enhanced by the use of cofactors.[1] Species such as flavins,[2] pyridoxal phosphate (PLP),[3] and cobalamin[4] are bound by their respective apoenzymes to form a holoenzyme complex that is capable of binding additional substrates, mediating their reactivity. The mechanism of action of biological cofactors has inspired many famous synthetic transformations over the years.[5]

While synthetic chemists are inspired by the innate mechanisms of cofactor-mediated catalysis, the molecular recognition aspects inspire supramolecular chemists.[6] This can motivate multiple avenues of research: external cofactors can be used to switch catalyst function or as allosteric effectors in a wide range of catalytic processes.[7] Alternatively, a small molecule cofactor can be bound *internally* in the host cavity, which then promotes a reaction between other species also bound in that site. This could be defined as "holoenzyme"-mimicry, in that the host active site mediates the reaction of a bound cofactor (such as PLP, flavin, etc.), enhancing rate and providing stereoselectivity. This requires binding multiple different species in a synthetic host[8] as well as activating the substrates and turning them over,[9] which is still a significant challenge for synthetic host species. Coencapsulation of two or more guests to form homoternary complexes is relatively well-known,[10] but formation of heteroternary complexes is rarer.[11] Additionally, most of these examples exhibit tight host/guest binding to allow coencapsulation, so turnover can be problematic, limiting their use as catalysts. Many supramolecular catalysts either promote unimolecular rearrange-

ments[12] or promote the dimerization of complementary substrates.[13] There are far fewer examples of "cofactor-mediated catalysis" with synthetic receptors, namely the use of a host/guest complex to catalyze reaction between *additional* reactants bound inside the parent host.

One strategy is to use a very small cofactor, namely a solvent-coordinated $H^+$ or $OH^-$ ion.[14] Alternatively, $M_4L_6$ catecholate hosts in water can bind organometallic species[15] and can effect small molecule transformations such as intermolecular cyclizations and isomerizations, among others.[16] Larger cofactors usually require supercapsules such as $Pd_{12}L_{24}$ and $Pd_{24}L_{48}$ nanospheres[17] or self-assembled resorcinarene hexamers,[18] which have interior cavity volumes of greater than 1375 Å$^3$.[19] This allows the binding of multiple small molecules in internal "nanophases" and has been used to promote either Brønsted acid[20] or gold catalyzed cyclization reactions,[21] iminium-catalyzed conjugate additions,[22] and carbonyl—olefin metatheses.[23] Other examples of hosts that can exploit cofactor effects are metalloporphyrin assemblies, which use ligand to the metal centers to control selectivity and rate in processes such as hydroformylation.[24]

One of the advantages of smaller, more defined host structures is that the size of the individual components can be varied to affect the reaction outcome: by changing the size and shape of the cofactor, different selectivities could be observed for different reactants. Smaller hosts can have their own issues

in supramolecular catalysis, however, most notably product inhibition and poor turnover.[25] Here, we show that an organic-soluble metal−ligand cage complex can act as a host environment for cofactor-mediated catalysis. The cage is a promiscuous, yet high affinity host, and multiple guests can be bound, reacted and released. The reaction kinetics depend on the molecular recognition of all the components in the reaction, and small changes in substrate structure can have large effects on the host-catalyzed reaction.

## ■ RESULTS AND DISCUSSION

We recently synthesized the large tetrahedral $Fe_4L_6$ cage complexes **1** and **2** (Figure 1).[26] Acid-functionalized cage **2** is an effective biomimetic catalyst, capable of catalyzing sequential tandem reactions[26] and nucleophilic substitutions such as the thioetherification of triphenylmethanol.[27] This process involves the formation of ternary host/guest complexes and hints at the possibility of cofactor-mediated catalysis in synthetic receptors. As the thioetherification of triphenylme-

thanol **4a** with alkylmercaptans is well-suited for mechanistic analysis in these cage complexes, we initially tested whether unfunctionalized cage **1** could promote the reaction in the presence of a suitably sized acidic cofactor.

The initial tests were performed with the fluorene-based diacid **3a**, a direct synthetic precursor to acid cage **2**. Triphenylmethanol **4a** was heated with 1.25 molar equiv of *n*-propanethiol in the presence of 5% cage **1** and 30% cofactor **3a** in $CD_3CN$, and the initial rate of the reaction forming thioether **5a** was monitored by ^{1}H NMR (Figure 2).
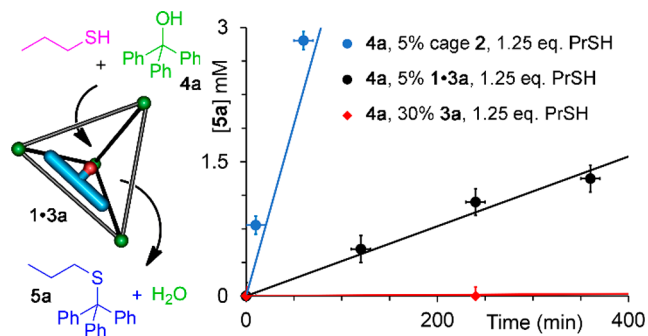
**Figure 2.** Cofactor-mediated catalysis with cage **1** and acid **3a**. Reaction progress over time for the thioetherification of electrophile **4a** with PrSH and either 5% cage **2**, 5% cage **1**/30% **3a**, or 30% **3a** alone as catalyst. [**4a**] = 15.8 mM, [PrSH] = 19.8 mM, reactions were performed at 80 °C in $CD_3CN$.

Interestingly, the combination of **1** and **3a** is an effective catalyst for the reaction, showing a >50-fold increase in initial rate when compared to the same concentration of **3a** in the absence of **1**. The process is *not* catalyzed by cage **1** in the absence of catalyst at all. The rate of the cofactor-mediated process with **1·3a** is ∼30 times slower than the reaction catalyzed by 5% acid-functionalized cage **2**,[27] as might be expected, but this initial experiment illustrates that the presence of cage **1** can significantly enhance the activity of the free acid catalyst, despite the fact it has no reactive functional groups. This suggests that molecular recognition effects are involved, and the acid is indeed acting as a "cofactor", and the cage as a holoenzyme mimic. Importantly, cage **1** is stable to the presence of acid **3a**, and no decomposition is seen during the reaction, even after 12 h at reflux in $CD_3CN$ (Figure S4). It is intolerant to stronger acids (e.g., camphorsulfonic acid (CSA) or $CF_3CO_2H$[26]) at high temperatures, however. Rapid decomposition and solvolysis of the iminopyridine groups is seen in the presence of 6 equiv of CSA after 5 min at 80 °C in $CD_3CN$.

To determine whether the accelerated reaction with **1·3a** was due to molecular recognition, we investigated the guest binding properties of cage **1** in more detail. We have previously shown that these extended fluorenyl cages, notably acid-functionalized cage **2**, show strong binding affinities (up to 200000 $M^{-1}$) for small molecules in acetonitrile.[26,27] Unfunctionalized cage **1** has a substantially larger cavity than acid cage **2**, however, and cannot exploit polar interactions between the host COOH groups and guest. In addition, the lack of bulky acid groups creates larger "gaps" between the walls of the cage (Figures 1b, 1c), which should lower guest affinity, especially for small neutral species.

Analysis of the host properties of cage **1** is not trivial. The interior cavity of **1** is large (∼600 Å$^3$), and all of the
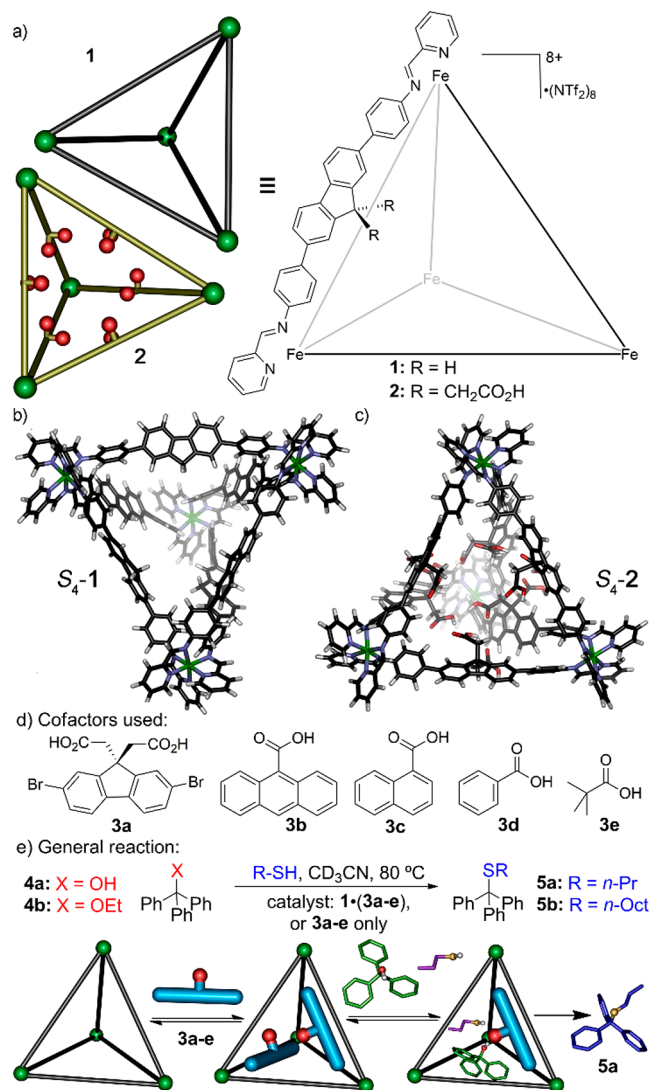
**Figure 1.** (a) Structures of $Fe_4L_6$ cage **1** and acid-decorated cage **2**.[26] Minimized structures of the $S_4$ isomers of (b) cage **1**; (c) cage **2** (SPARTAN, Hartree−Fock); (d) structures of the acid cofactors; (e) summary of the acid catalyzed substitution processes tested (**1·(3a−e)** = 1:6 ratio of cage: cofactor).

components are small enough to theoretically form ternary (or in some cases higher) complexes with **1**. The gaps between the ligand walls are also large, and all guests tested show fast in/out exchange rates on the NMR time scale. Chemical shift changes of protons in either the guest or the host in $^1$H NMR experiments are small, and the fact that cage **1** exists as a mixture of three metal-centered isomers in solution (48% $C_3$, 41% $S_4$, 11% $T$)[26] only adds to the complexity. The high freezing point of $CD_3CN$ limits low-temperature investigations, and the exchange rates are too fast to allow effective NOE buildup in 2D NMR experiments. Fortunately, UV/vis absorbance titrations are an effective method of investigating the recognition events. The binding constants are high enough that strong changes in absorbance of cage **1** occur at even micromolar concentrations in $CH_3CN$. Each guest was titrated into a 1.5 μM solution of **1** in $CH_3CN$, and the changes in absorbance at both 330 and 370 nm were recorded and analyzed. The binding isotherms were fit with both 1:1 and 1:2 models,[28] and we then analyzed the best fit for each guest. The results are summarized in Table 1; for the full fitting details, including fitting curves, variances, and error analysis, see the Supporting Information.

**Table 1. Binding Affinities of Reaction Components in Cage 1**[a]



| 1:2 substrate | $K_1 \times 10^3$ M$^{-1}$ | $K_2 \times 10^3$ M$^{-1}$ | $\alpha$ ($4K_2/K_1$)[28a] |
|---|---|---|---|
| OctSH | 174 ± 43 | 0.78 ± 0.53 | 0.018 |
| ether **4b** | 47.1 ± 8.5 | 2.11 ± 0.38 | 0.18 |
| acid **3a** | 19.0 ± 11 | 244 ± 89 | 51 |
| 1:1 substrate | $K_a \times 10^3$ M$^{-1}$ | | $K_a \times 10^3$ M$^{-1}$ |
| PrSH | 58.5 ± 4.7 | alcohol **4a** | 14.5 ± 0.77 |
| acid **3b** | 95.4 ± 5.5 | thioether **5a** | 24.8 ± 1.5 |
| acid **3c** | 102 ± 5.2 | thioether **5b** | 91.7 ± 7.8 |
| acid **3d** | 25.5 ± 1.0 | (OctS)$_2$ | 76.1 ± 3.8 |
| acid **3e** | 2.40 ± 0.15 | | |

[a]In $CH_3CN$, [**1**] = 1.5 μM, absorbance changes measured at 300/330 nm and 370 nm.[28]

Twelve different components (Figure 1d) were analyzed that would allow a range of mechanistic investigations into the thioetherification reaction. They consisted of two trityl electrophiles **4a** and **4b**, two different sized nucleophiles *n*-propanethiol (PrSH) and *n*-octanethiol (OctSH), five acidic cofactors **3a–e**, as well as the thioether products **5a** and **5b** and dioctyl disulfide (OctS)$_2$. All of the components show strong affinity for the cage, interestingly, even small species such as PrSH. In each case, the binding isotherms were fit to both the 1:1 and unbiased 1:2 binding models and the variances calculated. The significance of the 1:2 model was judged based on the inverse ratio of the squared residuals compared to the 1:1 model and quantified via their *p* value. Three general patterns emerged from this analysis, and these are summarized in Table 1 (and Tables S2–S4). Three guests unambiguously showed best fit to the 1:2 binding model, with *p* values below 0.001, and are labeled as the 1:2 substrates in Table 1: OctSH, trityl ether **3b**, and cofactor **3a**. In these cases,

two equilibrium constants were extracted, defined as $K_1$ and $K_2$, illustrating the sequential formation of 1:1 and 1:2 host/guest complexes.

The calculated binding affinities are all strong, with the weakest affinity shown by pivalic acid **3e**. Every other guest has an affinity of >10$^4$ M$^{-1}$, which corresponds to >95% occupancy at millimolar concentrations, so competitive guest binding effects are clearly relevant in any catalytic process. The larger guests show greater affinities, as might be expected, and anthroic/naphthoic acids **3b** and **3c** are very strongly bound, with affinities of ~100000 M$^{-1}$. Notably, the thioethers **5a** and **5b** are strongly bound as well, indicating that product inhibition is a factor that must be considered in any cage-catalyzed reactions with **1**. Unfortunately, the complex fitting equations prevent unambiguous proof of 1:2 *hetero*complexes with multiple different guests. Titration of **3a** into **1·PrSH** shows additional changes in absorbance, but it is not possible to determine whether this is due to expulsion of PrSH or formation of heteroternary complexes.

The substrates that form 1:2 complexes are especially interesting. As the 1:2 binding model was unbiased, the cooperativity of the binding process was not assumed in the model, and the cooperativity factor $\alpha$ (defined as $4K_2/K_1$) can be analyzed.[28a] Interestingly, the cooperativity of the 1:2 substrates is not constant. While OctSH and ether **3b** show negative cooperativity ($\alpha < 1$), diacid cofactor **3a** shows strong *positive* cooperativity, with $\alpha$ = 51. This is presumably due to self-complementary hydrogen bonds between the two diacids, but why this is not seen for the other acids **3b–3e** is not clear. Molecular modeling sheds some light on the binding modes. The large guests fill the space on the interior quite effectively in a 1:2 manner: the minimized structures of **1·3a$_2$** and **1·4b$_2$** (SPARTAN, Hartree–Fock) are shown in Figure 3a,b. The cavity is easily spacious enough to occupy two guests, and the relatively large exit/entry portals can allow fast guest exchange.
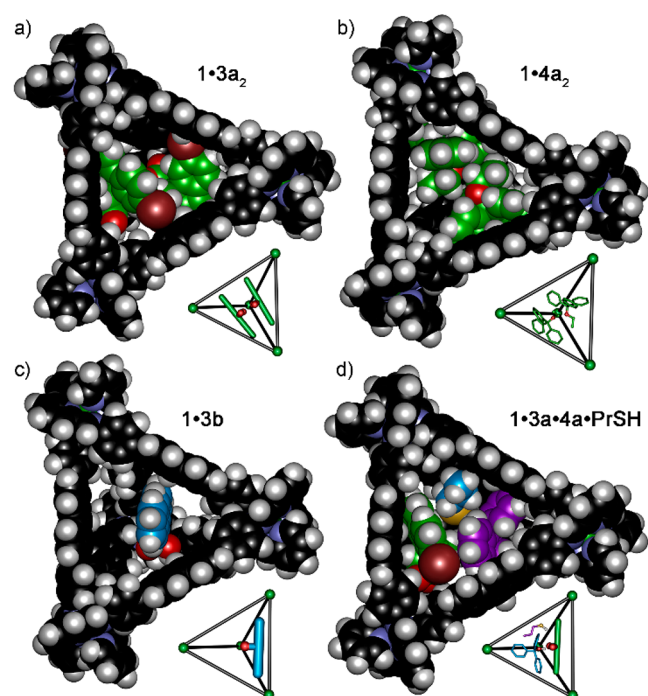


**Figure 3.** Minimized structures (SPARTAN, Hartree–Fock) of (a) $S_4$-**1·3a$_2$**; (b) $S_4$-**1·4a$_2$**; (c) $S_4$-**1·3b**; and (d) $S_4$-**1·3b·4a·PrSH**.

214 The cavity is even large enough to conceivably form a
215 quaternary complex with all three reactants (Figure 3d),
216 although this would have substantial entropic penalties. This,
217 of course, introduces the question of why there is observable
218 affinity for all the guests, and at such high binding constants,
219 even for small guests such as PrSH. The **1·3b** complex in
220 Figure 3c illustrates the large spaces in the cavity upon binding
221 only one guest. Obviously the remainder of the cavity can be
222 filled by solvent molecules, but Rebek's 55% occupancy rule is
223 not dominant here.[29] The most reasonable suggestion is that
224 the small, polar guests interact with the octacationic cage and
225 its aromatic walls via CH−π and π−π interactions, and these
226 interactions allow transient formation of host/guest complexes.
227 This is not unprecedented: the Nitschke lab has shown that a
228 variety of Fe−iminopyridine cages with large cavities can show
229 rapid in/out kinetics with small molecule guests,[30] and only
230 when the exit portals are reduced in size do kinetically stable
231 Michaelis complexes form. It is important to note that accurate
232 structural information about *where* the guests reside complexes
233 is still lacking, due to the limited information available from
234 NMR analysis. These cages have no large flat panels creating a
235 boxlike enclosure;[15a,30] rather, the walls are very much edge-
236 oriented and so the usual definition of guests being "inside" or
237 "outside"[30a] the cage is less clear. The models in Figure 3 are
238 plausible representations of host/guest complexes but are not
239 the only possibilities that would allow promoted reaction.
240 What is clear from the binding studies is that the host brings
241 multiple species into close proximity, which allows accelerated
242 reactions.

243 Having illustrated the binding affinity of the various
244 components, we investigated the effect of the cage on the
245 kinetics of the various acid-catalyzed thioetherification
246 processes. The components of the reaction were systematically
247 varied, focusing on small changes in component structure that
248 should have minimal effects on the reaction in the absence of
249 cage. The two electrophiles triphenylmethanol **4a** and its ethyl
250 ether **4b** have similar reactivities and only small differences in
251 size. The five different acid cofactors (**3a–e**, Figure 1) were
252 chosen such that the size of the cofactor could be varied
253 significantly while retaining relatively similar acidities. The
254 inspiration for the process, diacid **3a**, is the largest substrate
255 and has a p$K_a$ of ∼3.7 (based on comparison with 3,3-
256 dimethylglutarate[31]). The other cofactors vary slightly in p$K_a$
257 (**3b** = 3.65, **3c** = 3.69, **3d** = 4.20, **3e** = 5.03)[31] but have
258 substantial differences in volume (**3a** = 244 Å³, **3b** = 159 Å³, **3c**
259 = 122 Å³, **3d** = 96 Å³, **3e** = 84 Å³). Finally, the two
260 nucleophiles PrSH and OctSH show highly similar nucleo-
261 philicity but significantly different overall size, with volumes of
262 68 and 136 Å³, respectively.

263 The first tests were to determine the effect of varying the
264 cofactor catalyst, keeping the nucleophile and electrophile
265 constant (alcohol **4a** and PrSH, respectively). The ratio of
266 cage/cofactor was kept constant at 5% cage **1** and 30% cofactor
267 **3a–e**, with [**4a**] = 15.8 mM in CD₃CN. This 1:6 ratio of cage
268 to cofactor will be described as **1·3a–e** for the rest of this
269 paper. The reactions were run to ∼25% completion to ensure
270 accuracy in initial rate measurement (although some of the
271 faster reactions proceeded further in the same time frame).
272 The initial rates for the cage-mediated processes (V(**1·3a–e**))
273 and the background rate with 30% cofactor in the absence of
274 cage (V(**3a–e**)) are shown in Table 2 and Figure 4. The
275 different cofactors show quite different catalytic activities, even
276 in the absence of cage. The reaction rates catalyzed by "free"

**Table 2. Supramolecular Cofactor-Mediated Catalysis**[a]

| acid cofactor | V(**1·(3a–e)**) × 10⁻⁴ mM/min | V(**3a–e**) × 10⁻⁴ mM/min | V(**1·3(a–e)**)/ V(**3a–e**) |
|---|---|---|---|
| **3a** | 39 | 0.7 | 56 |
| **3b** | 229 | 19 | 12 |
| **3c** | 126 | 67 | 1.9 |
| **3d** | 109 | 33 | 3.3 |
| **3e** | 92 | 8 | 12 |

[a][**4a**] = 15.8 mM, [RSH] = 19.8 mM, reactions were performed at 80 °C in CD₃CN. Initial rates were determined using the first set of linear time points under 50% conversion by comparing Δ[**5a**]/t (min). Concentrations were confirmed using dioxane as a standard (7.9 mM).
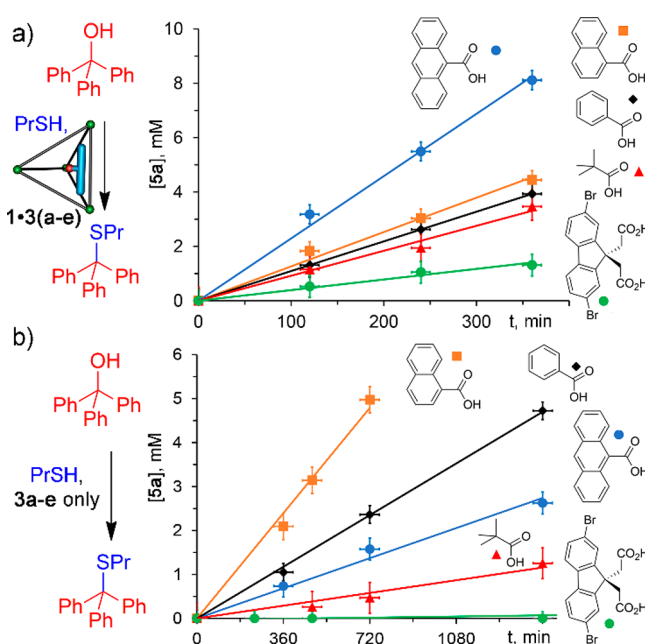


**Figure 4.** Dependence on cofactor size. Reaction progress over time for the thioetherification of electrophile **4a** and **4b** with PrSH (a) 5% cage **1**/30% cofactor **3a–e** catalyst and (b) 30% **3a–e** alone. [**4a**] = 15.8 mM, reactions were performed at 80 °C in CD₃CN.

cofactors **3a–e** vary somewhat, but they do not follow the 277
trend of p$K_a$; naphthoic acid **3c** is the best catalyst, and diacid 278
**3a** is by far the worst, despite their similar p$K_a$'s. The relative 279
order of effectiveness is **3c** > **3d** > **3b** ≫ **3e** > **3a**. None of the 280
free catalysts **3a–e** are particularly effective, however, with all 281
of the reactions only reaching <30% conversion at best after 6 282
h reflux. In each case, the reactions were very clean: the only 283
observed species in the NMR were the reactants, thioether 284
products, and a small amount of disulfide (see below) in 285
certain cases. No ester byproducts from tritylation of the acids 286
were seen, either in the control or cage-catalyzed examples. 287

When 5% cage **1** is added, the relative rates of reaction 288
change markedly, and the rate acceleration due to the presence 289
of catalytic cage **1** varies significantly with the nature of the 290
acid cofactor. The overall reaction rate order is **1·3b** > **1·3c** ∼ 291
**1·3d** > **1·3e** > **1·3a**. Addition of cage **1** has the largest effect on 292
the reactions catalyzed by diacid **3a**, anthroic acid **3b**, and 293
pivalic acid **3e**, with each complex showing at least a 10−50- 294

fold enhancement in initial rate compared to that with the free acid. In contrast, the reactions catalyzed by naphthoic acid **3c** and benzoic acid **3d** are only accelerated ~2-fold by the presence of 5% cage **1**. In addition, simply varying the cofactor in the cage-mediated process from **3a** and **3b** causes a 15-fold rate difference, despite the fact that the cofactor $pK_a$'s are essentially the same and all other conditions are identical. The thioetherification process caused no decomposition of the cage (Figure S4), even under extended reaction times, but some oxidative dimerization of the PrSH nucleophile was observed in the slower reactions, presumably caused by small amounts of free $Fe^{II}$ leached from the cage and atmospheric oxygen. This reaction was slower than the thioetherification reaction, and only small amounts of $(PrS)_2$ were observed. Interestingly, this small amount of free Lewis acid is not capable of catalyzing the thioetherification: no reaction was observed after extensive heating with **1** alone.

The next steps were to investigate which components were directly involved in the rate equation: while the thioether-ification reaction with "free" catalyst is an $S_N1$ process and will have no dependence on [nucleophile], introducing the cage **1** host into the reaction will change this. If the cofactor, electrophile, and/or nucleophile are bound by the cage before the rate-determining step, the reaction rate will show a dependence on [nucleophile]. We therefore performed initial rate studies with varying electrophile type (**4a** or **4b**), varying [cofactor], and varying concentration and size of nucleophile (Figures 5 and 6). For simplicity, we narrowed down the focus to the cofactors that were most strongly affected by the presence of cage **1**, diacid **3a**, and anthroic acid **3b**.

The relevant questions are whether the reaction rate is dependent on the concentration of cofactor and/or nucleo-phile and how this dependence changes upon varying the nature of the electrophile between alcohol **4a** and ether **4b**. The reaction rate is indeed dependent on [cofactor], as might
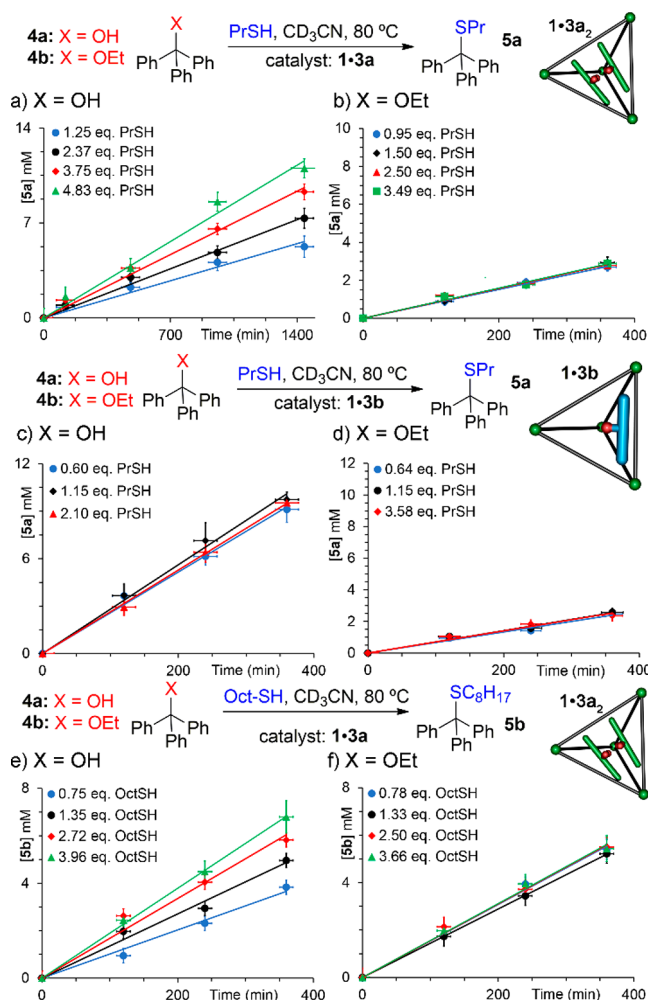
**Figure 6.** Reaction dependence on nucleophile concentration and size. Reaction progress over time with (a) **4a**, varying [PrSH], **1·3a** catalyst; (b) **4b**, varying [PrSH], **1·3a** catalyst; (c) **4a**, varying [PrSH], **1·3b** catalyst; (d) **4b**, varying [PrSH], **1·3b** catalyst; (e) **4a**, varying [OctSH], **1·3a** catalyst; (f) **4b**, varying [OctSH], **1·3a** catalyst. [**4a**, **4b**] = 15.8 mM, [**1**] = 0.8 mM, [**3a**, **3b**] = 4.8 mM. Reactions were performed at 80 °C in $CD_3CN$.
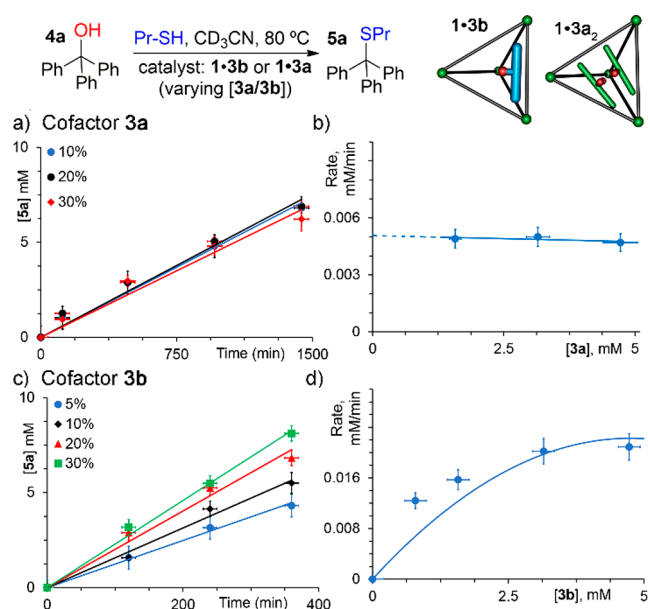
**Figure 5.** Reaction dependence on cofactor concentration: (a) reaction progress over time with varying [**3a**]; (b) reaction rate vs [**3a**]; (c) reaction progress over time with varying [**3d**]; (d) reaction rate vs [**3b**]. [**4a**] = 15.8 mM, [PrSH] = 19.8 mM, reactions were performed at 80 °C in $CD_3CN$.

be expected; Figure 5 shows the variation in initial rate upon varying [**3a**] or [**3b**] from 1.6 to 4.8 mM (10−30% with respect to electrophile) while keeping the [**1**] constant at 15.8 mM, and the reaction rate increases with increasing [**3b**]. The observations are somewhat surprising: the rate of the acid-catalyzed reaction is not affected by variations in concentration of diacid **3a**. The acid must be involved in the reaction, as the process does not occur without it, nor can it be catalyzed by cage **1** in the absence of acid. The explanation lies in the unusual binding characteristics of diacid **3a**: as the binding is strongly positively cooperative ($\alpha$ = 51), the resting state is **1·3a_2**, not **1·3a**. As the binding is so high, even at a 1:1 cage/guest ratio, the inactive **1·3a_2** dominates the resting state, so the rate is essentially independent of **3a**. In contrast, anthroic acid **3b**, which binds in a 1:1 manner, shows saturation kinetics, with rate increasing with increasing [**3b**] but slowing at high [**3b**]. This is likely due to inhibition by saturating the cage with excess cofactor **3b**. This reactivity profile indicates the possibility of forming **1·3b_2**, as was hinted at by the fitting analysis. If a small amount of **1·3b_2** can form, it is not positively

cooperative, and the resting and active states of the cage/cofactor complex are identical.

The other unusual observation is that the putatively "$S_N1$" reaction to form thioether **5a** shows variable rate dependences when the components are varied, including showing rate dependence on the concentration of *nucleophile*. When small molecules are used to catalyze this reaction, no rate dependence on nucleophile is seen:[27] only when cage catalysts capable of molecular recognition (such as **2**) are used. Figure 6 shows the initial rates observed for the cage-catalyzed thioetherification reaction at varying concentrations of nucleophile. The six entries in Figure 6 show these effects on reactions between electrophiles **4a** and **4b**, with PrSH and OctSH nucleophiles, and with cofactors **3a** and **3b**. Even at first glance, it is obvious that small changes in reactant structure effect large changes in rate and dependence on [nucleophile] in the cage-catalyzed reaction.

Figure 6a clearly shows that the rate of reaction between **4a** and PrSH catalyzed by the **1·3a** complex is dependent on [PrSH]. The rate at [PrSH] = 19.8 mM was $39 \times 10^{-4}$ mM/min. When ether **4b** was subjected to the same conditions, the observed rate was slightly faster at $79 \times 10^{-4}$ mM/min. However, upon changing the concentration of PrSH, the rate of reaction of ether **4b** remains identical, whereas that with alcohol **4a** increases significantly with increasing [PrSH]. This variation in dependence on nucleophile concentration is not due to differing mechanisms of reaction between **4a** and **4b** in the absence of cage: using either strong acids such as $CF_3CO_2H$[27] as catalyst shows no change in rate with varying [PrSH], as would be expected for an $S_N1$ reaction. The structural change in electrophile is small—there is a difference in basicity between **4a** and **4b** (conjugated acid $pK_a$ of $\sim-3.5$ vs $-2$) as well as a small difference in size, but the cation formed upon reaction is identical, so the change in [nucleophile] dependency is unusual. This observation mirrors the effect seen with acid-functionalized cage **2**,[27] where molecular recognition effects change the molecularity of the reaction. In this case, similar changes in nucleophile dependence are observed for a cofactor-mediated process.

When anthroic acid **3b** is used as cofactor, the kinetic behavior of the reaction changes significantly. The rate of reaction of alcohol **4a** with PrSH catalyzed by **1·3b** is much faster ($260 \times 10^{-4}$ mM/min) than with **1·3a**, whereas the reaction rate with ether **4b** is essentially unchanged ($70 \times 10^{-4}$ mM/min). In both cases catalyzed by **1·3b**, there is no dependence on [PrSH]. Finally, the nature of the nucleophile was varied, and the larger *n*-octanethiol (OctSH) was used in place of PrSH. Parts e and f of Figure 6 show the rate profiles for the reaction of OctSH with electrophiles **4a** and **4b**, with **1·3a** as catalyst. The initial rates of thioetherification are faster than those with PrSH ($k(\mathbf{4a}) = 135 \times 10^{-4}$ mM/min, $k(\mathbf{4b}) = 150 \times 10^{-4}$ mM/min with 1.25 equiv of OctSH). The dependence on nucleophile concentration is similar to that shown by PrSH: ether **4b** has no dependence on [OctSH], whereas alcohol **4a** does.

In addition to the differences in thioetherification rate, the reaction with OctSH displayed one other notable difference from that with PrSH: OctSH is oxidatively dimerized to the disulfide $(OctS)_2$ by cage **1** at a much faster rate. We have previously observed that more reactive aryl thiols can be oxidized to the disulfides by Fe-containing cages,[27] but oxidation of alkyl thiols is very sluggish. Despite the two

thiols having highly similar oxidation potential, OctSH was oxidized by 5% cage **1** at a rate 4-fold faster than PrSH.

The presence of the cage has a variety of effects on the reactions, some subtle and some that are quite remarkable. Figure 7 shows a summary of some of the effects of the cage on
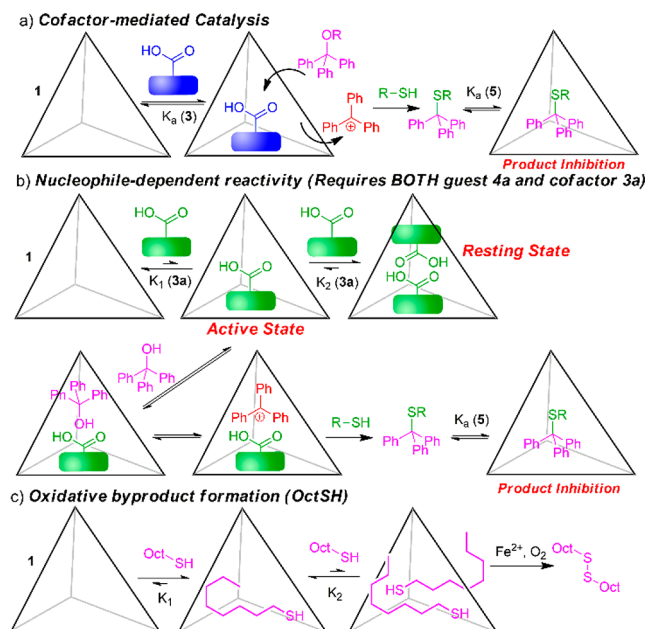
**Figure 7.** Mechanistic possibilities in the cofactor-mediated process: (a) "standard" cofactor-mediated process; (b) requirements for nucleophile-dependent kinetics; (c) accelerated dimerization of large nucleophiles by favorable ternary complex formation.

the reaction process. Not all of the possible equilibria are shown, for clarity; as there are as many as four components in the reaction mixture as well as the cage, and as some of them can form 1:1 and 1:2 homo- and heteroternary complexes, there are many possible host/guest processes occurring during the reaction. Despite the host showing strong affinity for all components of the reaction, the rapid in/out exchange rates of the substrates allow the cofactor-mediated catalysis to be successful.

The general accelerated cofactor-mediated process is illustrated in Figure 7a, covering the reactions that do not show nucleophile dependence (e.g., with **4b**, **3b**, etc.). In this case, a standard $S_N1$ mechanism is occurring, and cation formation is the rate-determining step. The electrophile and cofactor can each bind in the cavity of **1**, and the accelerated reaction occurs when the electrophile **4** is activated by the **1·3** complex. The rate acceleration is controlled by the relative proportion of the **1·3·4** complex in solution. This is not dependent on the affinity of the individual components: for example, naphthoic acid **3c** has essentially the same affinity for **1** as anthroic acid **3b** but gives only a 2-fold acceleration of the **4a**/PrSH thioetherification, as opposed to a 12-fold acceleration with **3b**. The strongest accelerations are seen with reactants that show synergistic coencapsulation in the host cavity. It should be noted that the products **5a**/**5b** have stronger affinity for **1** than the reactants, and some product inhibition is observed at high conversions, in contrast with acid cage **2**, where the products has a lower affinity than the reactants.[27]

The most unusual reactivity is shown by the combination of cofactor **3a** and electrophile **4a** (Figure 7b). Whereas all other combinations showed $S_N1$-type kinetics, with the cage controlling the overall rate, using diacid **3a** as cofactor with triphenylmethanol showed a rate *independent* of cofactor concentration as well as dependent on nucleophile concentration. As discussed previously, the unique positive cooperativity in forming the **1·3a₂** complex can explain the lack of dependence on cofactor concentration with **3a**. The reasons for dependence on [nucleophile] are less obvious. With acid-bearing cage **2**, strong dependence on [nucleophile] was observed,[27] but that only requires formation of ternary host/guest complexes. For the cofactor-mediated process with cage **1**, introducing nucleophile before the rate-determining step would require the formation, however briefly, of a quaternary **1·3a·4a·PrSH** complex. The molecular modeling in Figure 3d suggests that this is plausible, as all three components can fit in the cavity of **1**. The entropic penalty of forming a quaternary complex could be overcome by expulsion of solvent molecules from the cavity. Other arguments could be made for pre-equilibrium binding of nucleophile in **1** affecting the rate, but as all other combinations show no nucleophile dependence, this is unlikely. The oddity is that the combination of **3a** and **4a** is unique—only in this case is nucleophile dependence seen, and this combination shows a much larger rate acceleration than with the other cofactors. The most likely reason is that the effects causing the positive cooperativity in formation of **1·3a₂** (self-complementary H-bonding with the diacid) also favor the formation of heteroternary complexes with the alcohol electrophile and can contribute to binding the nucleophile too. This phenomenon does require further investigation, however.

Finally, the competing oxidative dimerization of the nucleophile is an interesting illustration of the favorable 1:2 binding of the longer OctSH in cage **1** (Figure 7c). The accelerated dimerization of OctSH can be easily explained by the colocalization of the two thiols in the cage interior, with the reaction promoted by small amounts of free Fe$^{II}$ salts. PrSH is smaller and does not favor 1:2 complexes; hence, the dimerization rate is slower.

## ■ CONCLUSIONS

In conclusion, we have shown that a self-assembled Fe₄L₆ cage is capable of co-encapsulating multiple carboxylic acid containing guests in its cavity, and these acids can act as cofactors for cage-catalyzed nucleophilic substitutions. The most important observations are the nonlinear dependency of the reaction on cofactor concentration, the differing rate accelerations for differently sized cofactors and the variable dependency of the reaction nucleophile concentration. These observations illustrate that molecular recognition of one or more reaction components is key to the reaction outcomes. Small changes in the size and shape of the reactants and catalysts can have large effects on the reaction profile in unexpected ways. Differently sized cofactors, nucleophiles, and electrophiles all affect the reaction rate and molecularity differently, even when they have similar reactive properties outside the cage.

## ■ EXPERIMENTAL SECTION

**General Information.** Cages **1** and **2** and cofactor **3a** were synthesized according to literature procedures.[26] See that publication for full characterization. $^1$H and $^{13}$C spectra were recorded on Bruker Avance NEO 400 MHz or Bruker Avance 600 MHz NMR spectrometer. The spectrometers were automatically tuned and matched to the correct operating frequencies. Proton ($^1$H) and carbon ($^{13}$C) chemical shifts are reported in parts per million ($\delta$) with respect to tetramethylsilane (TMS, $\delta = 0$) and referenced internally with respect to the protio solvent impurity for CD₃CN ($^1$H: 1.94 ppm, $^{13}$C: 118.3 ppm). Deuterated NMR solvents were obtained from Cambridge Isotope Laboratories, Inc. (Andover, MA) and used without further purification. Spectra were digitally processed (phase and baseline corrections, integration, peak analysis) using Bruker Topspin 1.3 and MestreNova. All other materials were obtained from Aldrich Chemical Co. (St. Louis, MO) or Fisher Scientific (Fairlawn, NJ) and were used as received. Solvents were dried through a commercial solvent purification system (Pure Process Technologies, Inc.). UV/vis spectroscopy was performed on a Cary 60 photo-spectrometer using the Varian Scans program to collect data.

**Synthesis of Octyl Trityl Sulfide 5b.** Trityl chloride (100 mg, 0.36 mmol) was placed in a Schlenk flask with a stir bar and purged with N₂. *n*-Octanethiol (0.12 mL, 1.8 mmol) was added to the flask, and the reaction was stirred at 80 °C in a heating mantle for 12 h. The solvent was removed and the product dried in vacuo to yield pure product as a white crystalline solid (105.6 mg, 76%): $^1$H NMR (400 MHz, CD₃CN) $\delta$ 7.43 (dd, *J* = 5.6, 3.7 Hz, 6H), 7.35−7.31 (m, 6H), 7.28−7.24 (m, 3H), 2.3 (t, *J* = 7.4 Hz, 2H), 1.4−1.13 (m, 12H), 0.89 (t, *J* = 7.4 Hz, 3H); $^{13}$C {$^1$H} NMR (101 MHz, CD₃CN) $\delta$ 145.1, 129.4, 127.8, 126.6, 66.1, 31.5, 28.8, 28.7, 28.6, 28.2, 22.3, 13.4; HRMS (ESI-TOF) *m/z* calcd for C₂₇H₃₂S 388.2225, found 387.2141 ([M − H]⁻).

**General Procedure for Substitution Reactions.** Electrophile **4** (1 molar equiv, 6.3 μmol, 10 μL of 0.63 M solution) was placed in an NMR tube followed by 5 mol % cage **1** (0.31 μmol, 2 mg) and 30 mol % acid **3** (1.86 mmol, 5 μL of 0.372 M solution in CD₃CN) or 30% acid **3** alone. The nucleophile (1.25 molar equiv, 7.9 μmol, 3.9 μL of 2 M solution in CD₃CN) was then added followed by 1,4-dioxane as the internal standard (0.5 molar equiv, 3.2 μmol, 1.6 μL of 2 M solution in CD₃CN). A combined total volume of 400 μL of CD₃CN was added, and the tube was capped and quickly shaken to dissolve all solids. An initial $^1$H NMR spectrum of the reaction mixture was obtained to verify the stoichiometry of the sample. The sample was then heated at 80 °C and the reaction progress monitored over time. Rate calculation trials were performed in triplicate. The percent conversion values were obtained via integration of the product and substrate peaks against the internal standard, and the calculated values of repeated trials were averaged.

**General Procedure for Binding Affinity Calculations.** A 1.5 μM solution of cage **1** was prepared in spectroscopic-grade CH₃CN via dilutions from a 0.3 mM stock solution and added to a UV−vis cuvette. To this solution was then added 1 μL aliquots from a 4.5 mM solution of the corresponding guest molecule, equating to 1 molar equiv of guest to cage. These additions were continued until there was no observable change in the absorption spectrum. Binding affinities were calculated via linear regression analysis using the Nelder−Mead method from the change in absorbance at two points (300 nm/330 and 370 nm), the data were fit to either a 1:1 or 1:2 binding model, and the variance used to determine best fit using a nonlinear least-squares (maximum likelihood) approach written within the Mathematica programming environment.[28] See the Supporting Information for equations and a full description of the fitting.

## ■ ASSOCIATED CONTENT

### ⓢ Supporting Information

The Supporting Information is available free of charge on the ACS Publications website at DOI: 10.1021/acs.joc.9b01880.

Computational analysis of curve fittings (ZIP)

Binding analysis including spectroscopic data and binding isotherms, and kinetic data (PDF)

## ■ AUTHOR INFORMATION

**Corresponding Author**

*E-mail: richard.hooley@ucr.edu.

**ORCID**

Richard J. Hooley: 0000-0003-0033-8653

**Author Contributions**

[†]C.N. and P.M.B. contributed equally to the manuscript.

**Notes**

The authors declare no competing financial interest.

## ■ REFERENCES

(1) Richter, M. Functional diversity of organic molecule enzyme cofactors. *Nat. Prod. Rep.* **2013**, *30*, 1324−1345.

(2) Fagan, R. L.; Palfey, B. A. Flavin-dependent enzymes. *Comprehensive Natural Products II - Chemistry and Biology* **2010**, *7*, 37−113.

(3) Eliot, A. C.; Kirsch, J. F. Pyridoxal phosphate enzymes: mechanistic, structural, and evolutionary considerations. *Annu. Rev. Biochem.* **2004**, *73*, 383−415.

(4) Banerjee, R.; Ragsdale, S. W. The many faces of vitamin B12: catalysis by cobalamin-dependent enzymes. *Annu. Rev. Biochem.* **2003**, *72*, 209−247.

(5) (a) Kluger, R.; Tittmann, K. Thiamin diphosphate catalysis: enzymic and nonenzymic covalent intermediates. *Chem. Rev.* **2008**, *108*, 1797−1833. (b) Breslow, R. On the mechanism of thiamine action. IV.[1] Evidence from studies on model systems. *J. Am. Chem. Soc.* **1958**, *80*, 3719−3726. (c) Shinkai, S.; Ishikawa, Y.; Shinkai, H.; Tsuno, T.; Makishima, H.; Ueda, K.; Manabe, O. A crown ether flavin mimic: synthesis and properties of a flavin bearing a crown ring as a recognition site. *J. Am. Chem. Soc.* **1984**, *106*, 1801−1808. (d) Chevalier, Y.; Lock Toy Ki, Y.; le Nouen, D.; Mahy, J. P.; Goddard, J. P.; Avenier, F. Aerobic Baeyer−Villiger oxidation catalyzed by a flavin-containing enzyme mimic in water. *Angew. Chem., Int. Ed.* **2018**, *57*, 16412−16415.

(6) Dong, Z.; Luo, Q.; Liu, J. Artificial enzymes based on supramolecular scaffolds. *Chem. Soc. Rev.* **2012**, *41*, 7890−7908.

(7) (a) Lüning, U. Switchable catalysts. *Angew. Chem., Int. Ed.* **2012**, *51*, 8163−8165. (b) McConnell, A. J.; Wood, C. S.; Neelakandan, P. P.; Nitschke, J. R. Stimuli-responsive metal−ligand assemblies. *Chem. Rev.* **2015**, *115*, 7729−7793. (c) Blanco, V.; Leigh, D. A.; Marcos, V. Artificial switchable catalysts. *Chem. Soc. Rev.* **2015**, *44*, 5341−5370.

(8) (a) Rizzuto, F. J.; von Krbek, L. K. S.; Nitschke, J. R. Strategies for binding multiple guests in metal-organic cages. *Nat. Rev. Chem.* **2019**, *3*, 204−222. (b) Hof, F.; Craig, S. L.; Nuckolls, C.; Rebek, J., Jr. Molecular encapsulation. *Angew. Chem., Int. Ed.* **2002**, *41*, 1488−1508.

(9) Brown, C. J.; Toste, F. D.; Bergman, R. G.; Raymond, K. N. Supramolecular catalysis in metal-ligand cluster hosts. *Chem. Rev.* **2015**, *115*, 3012−3035.

(10) (a) Kang, J. M.; Rebek, J., Jr. Entropically driven binding in a self-assembling molecular capsule. *Nature* **1996**, *382*, 239−241. (b) Yamauchi, Y.; Yoshizawa, M.; Akita, M.; Fujita, M. Engineering double to quintuple stacks of a polarized aromatic in confined cavities. *J. Am. Chem. Soc.* **2010**, *132*, 960−966. (c) Yoshizawa, M.; Tamura, M.; Fujita, M. AND/OR bimolecular recognition. *J. Am. Chem. Soc.* **2004**, *126*, 6846−6847. (d) Samanta, D.; Gemen, J.; Chu, Z.; Diskin-Posner, Y.; Shimon, L. J. W.; Klajn, R. Reversible photoswitching of encapsulated azobenzenes in water. *Proc. Natl. Acad. Sci. U. S. A.* **2018**, *115*, 9379−9384.

(11) (a) Kang, J. M.; Rebek, J., Jr. Acceleration of a Diels-Alder reaction by a self-assembled molecular capsule. *Nature* **1997**, *385*, 50−52. (b) Chen, J.; Rebek, J., Jr. Selectivity in an encapsulated cycloaddition reaction. *Org. Lett.* **2002**, *4*, 327−329. (c) Sawada, T.; Fujita, M. A single Watson-Crick G•C base pair in water: Aqueous hydrogen bonds in hydrophobic cavities. *J. Am. Chem. Soc.* **2010**, *132*, 7194−7201. (d) Mahata, K.; Frischmann, P. D.; Würthner, F. Giant electroactive $M_4L_6$ tetrahedral host self-assembled with Fe(II) vertices and perylene bisimide dye edges. *J. Am. Chem. Soc.* **2013**, *135*, 15656−15661.

(12) Fiedler, D.; Bergman, R. G.; Raymond, K. N. Supramolecular catalysis of a unimolecular transformation: Aza-cope rearrangement within a self-assembled host. *Angew. Chem., Int. Ed.* **2004**, *43*, 6748−6755.

(13) (a) Yoshizawa, M.; Tamura, M.; Fujita, M. Diels-Alder in aqueous molecular hosts: Unusual regioselectivity and efficient catalysis. *Science* **2006**, *312*, 251−254. (b) Nishioka, Y.; Yamaguchi, T.; Yoshizawa, M.; Fujita, M. Unusual [2 + 4] and [2 + 2] cycloadditions of arenes in the confined cavity of self-assembled cages. *J. Am. Chem. Soc.* **2007**, *129*, 7000−7001. (c) Martí-Centelles, V.; Lawrence, A. L.; Lusby, P. J. High activity and efficient turnover by a simple, self-assembled artificial Diels-Alderase. *J. Am. Chem. Soc.* **2018**, *140*, 2862−2868.

(14) (a) Pluth, M. D.; Bergman, R. G.; Raymond, K. N. Acid catalysis in basic solution: A supramolecular host promotes orthoformate hydrolysis. *Science* **2007**, *316*, 85−88. (b) Cullen, W.; Misuraca, M. C.; Hunter, C. A.; Williams, N. H.; Ward, M. D. Highly efficient catalysis of the Kemp elimination in the cavity of a cubic coordination cage. *Nat. Chem.* **2016**, *8*, 231−236. (c) Cullen, W.; Metherell, A. J.; Wragg, A. B.; Taylor, C. G. P.; Williams, N. H.; Ward, M. D. Catalysis in a cationic coordination cage using a cavity-bound guest and surface-bound anions: inhibition, activation, and autocatalysis. *J. Am. Chem. Soc.* **2018**, *140*, 2821−2828.

(15) (a) Hong, C. M.; Bergman, R. G.; Raymond, K. N.; Toste, F. D. Self-assembled tetrahedral hosts as supramolecular catalysts. *Acc. Chem. Res.* **2018**, *51*, 2447−2455. (b) Kaphan, D. M.; Levin, M. D.; Bergman, R. G.; Raymond, K. N.; Toste, F. D. A supramolecular microenvironment strategy for transition metal catalysis. *Science* **2015**, *350*, 1235−1238.

(16) (a) Wang, J. Z.; Brown, C. J.; Bergman, R. G.; Raymond, K. N.; Toste, F. D. Hydroalkoxylation catalyzed by a gold(I) complex encapsulated in a supramolecular host. *J. Am. Chem. Soc.* **2011**, *133*, 7358−7360. (b) Levin, M. D.; Kaphan, D. M.; Hong, C. M.; Bergman, R. G.; Raymond, K. N.; Toste, F. D. Scope and mechanism of cooperativity at the intersection of organometallic and supramolecular catalysis. *J. Am. Chem. Soc.* **2016**, *138*, 9682−9693.

(17) Harris, K.; Fujita, D.; Fujita, M. Giant hollow $M_nL_{2n}$ spherical complexes: structure, functionalisation and applications. *Chem. Commun.* **2013**, *49*, 6703−6712.

(18) Zhang, Q.; Catti, L.; Tiefenbacher, K. Catalysis inside the hexameric resorcinarene capsule. *Acc. Chem. Res.* **2018**, *51*, 2107−2114.

(19) (a) MacGillivray, L. R.; Atwood, J. L. A chiral spherical molecular assembly held together by 60 hydrogen bonds. *Nature* **1997**, *389*, 469−472. (b) Shivanyuk, A.; Rebek, J., Jr. Reversible encapsulation by self-assembling resorcinarene subunits. *Proc. Natl. Acad. Sci. U. S. A.* **2001**, *98*, 7662−7665.

(20) (a) Zhang, Q.; Tiefenbacher, K. Terpene cyclization catalyzed inside a self-assembled cavity. *Nat. Chem.* **2015**, *7*, 197−202. (b) Zhang, Q.; Catti, L.; Pleiss, J.; Tiefenbacher, K. Terpene cyclizations inside a supramolecular catalyst: Leaving-group-controlled product selectivity and mechanistic studies. *J. Am. Chem. Soc.* **2017**, *139*, 11482−11492.

(21) (a) Gramage-Doria, R.; Hessels, J.; Leenders, S. H. A. M.; Tröppner, O.; Dürr, M.; Ivanović-Burmazović, I.; Reek, J. N. H. Gold(I) catalysis at extreme concentrations inside self-assembled nanospheres. *Angew. Chem., Int. Ed.* **2014**, *53*, 13380−13384. (b) Wang, Q.-Q.; Gonell, S.; Leenders, S. H. A. M.; Dürr, M.; Ivanović-Burmazović, I.; Reek, J. N. H. Self-assembled nanospheres

with multiple endohedral binding sites pre-organize catalysts and substrates for highly efficient reactions. *Nat. Chem.* **2016**, *8*, 225−230.

(22) Bräuer, T. M.; Zhang, Q.; Tiefenbacher, K. Iminium catalysis inside a self-assembled supramolecular capsule: Modulation of enantiomeric excess. *Angew. Chem., Int. Ed.* **2016**, *55*, 7698−7701.

(23) Catti, L.; Tiefenbacher, K. Brønsted acid-catalyzed carbonyl-olefin metathesis inside a self-assembled supramolecular host. *Angew. Chem., Int. Ed.* **2018**, *57*, 14589−14592.

(24) (a) Jongkind, L. J.; Elemans, J. A. A. W.; Reek, J. N. H. Cofactor controlled encapsulation of a rhodium hydroformylation catalyst. *Angew. Chem., Int. Ed.* **2019**, *58*, 2696−2699. (b) Nurttila, S. S.; Brenner, W.; Mosquera, J.; van Vliet, K. M.; Nitschke, J. R.; Reek, J. N. H. Size-selective hydroformylation by a rhodium catalyst confined in a supramolecular cage. *Chem.—Eur. J.* **2019**, *25*, 609−620.

(25) Hooley, R. J.; Biros, S. M.; Rebek, J., Jr. A deep, water-soluble cavitand acts as a phase-transfer catalyst for hydrophobic species. *Angew. Chem., Int. Ed.* **2006**, *45*, 3517−3519.

(26) Holloway, L. R.; Bogie, P. M.; Lyon, Y.; Ngai, C.; Miller, T. F.; Julian, R. R.; Hooley, R. J. Tandem reactivity of a self-assembled cage catalyst with endohedral acid groups. *J. Am. Chem. Soc.* **2018**, *140*, 8078−8081.

(27) Bogie, P. M.; Holloway, L. R.; Ngai, C.; Miller, T. F.; Grewal, D. K.; Hooley, R. J. A self-assembled cage with endohedral acid groups both catalyzes substitution reactions and controls their molecularity. *Chem.—Eur. J.* **2019**, *25*, 10232−10238.

(28) (a) Hibbert, D. B.; Thordarson, P. The death of the Job plot, transparency, open science and online tools, uncertainty estimation methods and other developments in supramolecular chemistry data analysis. *Chem. Commun.* **2016**, *52*, 12792−12805. (b) Thordarson, P. Determining association constants from titration experiments in supramolecular chemistry. *Chem. Soc. Rev.* **2011**, *40*, 1305−1323.

(29) Mecozzi, S.; Rebek, J., Jr. The 55% solution: a formula for molecular recognition in the liquid state. *Chem.—Eur. J.* **1998**, *4*, 1016−1022.

(30) (a) Rizzuto, F. J.; Carpenter, J. P.; Nitschke, J. R. Multisite binding of drugs and natural products in an entropically favorable, heteroleptic receptor. *J. Am. Chem. Soc.* **2019**, *141*, 9087−9095. (b) Meng, W.; Breiner, B.; Rissanen, K.; Thoburn, J. D.; Clegg, J. K.; Nitschke, J. R. A self-assembled $M_8L_6$ cubic cage that selectively encapsulates large aromatic guests. *Angew. Chem., Int. Ed.* **2011**, *50*, 3479−3483. (c) Ramsay, W. J.; Szczypiński, F. T.; Weissman, H.; Ronson, T. K.; Smulders, M. M. J.; Rybtchinski, B.; Nitschke, J. R. Designed enclosure enables guest binding within the 4200 Å$^3$ cavity of a self-assembled cube. *Angew. Chem., Int. Ed.* **2015**, *54*, 5636−5640.

(31) (a) Brown, H. C.; Braude, E. A.; Nachod, F.C. et al. *Determination of Organic Structures by Physical Methods*; Academic Press: New York, 1955. (b) Dippy, J. F. J.; Hughes, S. R. C.; Rozanski, A. The dissociation constants of some symmetrically disubstituted succinic acids. *J. Chem. Soc.* **1959**, 2492−2498.

I